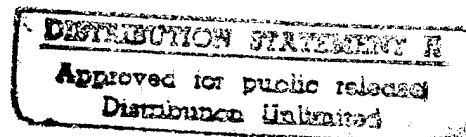


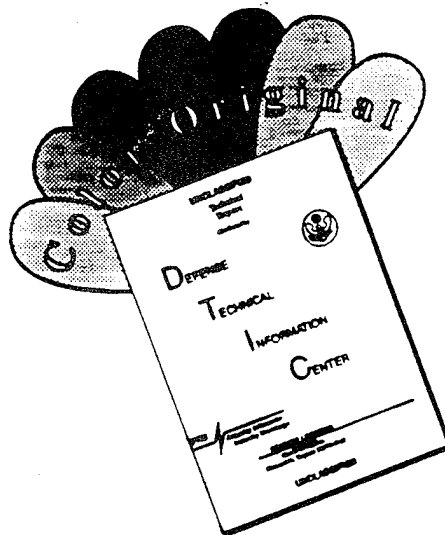
## REPORT DOCUMENTATION

1a. REPORT SECURITY CLASSIFICATION Unclassified		1b. RESTRICT	
2a. SECURITY CLASSIFICATION AUTHORITY		3. DISTRIBUTION / AVAILABILITY OF REPORT Unlimited Distribution	
2b. DECLASSIFICATION / DOWNGRADING SCHEDULE			
4. PERFORMING ORGANIZATION REPORT NUMBER(S)		5. MONITORING ORGANIZATION REPORT NUMBER(S)	
6a. NAME OF PERFORMING ORGANIZATION The Johns Hopkins University Applied Physics Laboratory	6b. OFFICE SYMBOL (If applicable)	7a. NAME OF MONITORING ORGANIZATION Directorate of Physics and Geophysical Sciences Air Force Office of Scientific Research	
6c. ADDRESS (City, State, and ZIP Code) Laurel, Maryland 20723		7b. ADDRESS (City, State, and ZIP Code) Bldg 410, Bolling AFB Washington, DC 20323-6448	
8a. NAME OF FUNDING / SPONSORING ORGANIZATION Air Force Office of Scientific Research	8b. OFFICE SYMBOL (If applicable) NH	9. PROCUREMENT INSTRUMENT IDENTIFICATION NUMBER F49620-92-5-0196	
8c. ADDRESS (City, State, and ZIP Code) 116 DUNCAN AVE, SUITE B115 BOLLING AFB DC 20332-0001		10. SOURCE OF FUNDING NUMBERS	
		PROGRAM ELEMENT NO. 61102 F	PROJECT NO. 2311
		TASK NO. AS	WORK UNIT ACCESSION NO.
11. TITLE (Include Security Classification) Final Technical Report: AFOSR Grant F49620-92-5-0196			
12. PERSONAL AUTHOR(S) Ching Meng			
13a. TYPE OF REPORT Final	13b. TIME COVERED FROM 1/1/92 TO 10/1/95	14. DATE OF REPORT (Year, Month, Day) January 3, 1996	15. PAGE COUNT 20 pages
16. SUPPLEMENTARY NOTATION			
17. COSATI CODES		18. SUBJECT TERMS (Continue on reverse if necessary and identify by block number)	
FIELD	GROUP	SUB-GROUP	
19. ABSTRACT (Continue on reverse if necessary and identify by block number)  A final report on research conducted under AFOSR Grant 92-5-0196 is given. New scientific results and techniques developed towards an understanding of the Earth's space environment are given.			
20. DISTRIBUTION / AVAILABILITY OF ABSTRACT <input checked="" type="checkbox"/> UNCLASSIFIED/UNLIMITED <input type="checkbox"/> SAME AS RPT. <input type="checkbox"/> DTIC USERS		21. ABSTRACT SECURITY CLASSIFICATION Unclassified	
22a. NAME OF RESPONSIBLE INDIVIDUAL Unclassified		22b. TELEPHONE (Include Area Code) 202-767-7901	22c. OFFICE SYMBOL NH



19960520 004

# DISCLAIMER NOTICE



THIS DOCUMENT IS BEST QUALITY AVAILABLE. THE COPY FURNISHED TO DTIC CONTAINED A SIGNIFICANT NUMBER OF COLOR PAGES WHICH DO NOT REPRODUCE LEGIBLY ON BLACK AND WHITE MICROFICHE.

**FINAL TECHNICAL REPORT: AFOSR GRANT F49620-92-J-0196  
"MAGNETOSPHERIC MORPHOLOGY AND DYNAMICS:  
SPECIFICATION OF THE NEAR-EARTH OPERATIONAL  
ENVIRONMENT"**

Principal Investigator: Ching-I. Meng

The Johns Hopkins University Applied Physics Laboratory

Covering AFOSR sponsored research from 1992-1995

## 1. Introduction and Overview

The goal of our research is to be able to monitor, understand, and ultimately forecast the behavior of the space plasma regimes surrounding the Earth. The first step in the procedure, accomplished in 1988-1991, was a series of papers on the identification of the sources (such as the shocked solar wind) of the dayside regions of precipitation into the ionosphere as accurately as possible from the DMSP series low-altitude satellites. The identification were then automated [Newell *et al.*, 1991], allowing massive statistical studies. The second step, funded by this AFOSR grant and carried out in 1992-1995 using the capabilities created by the first step, has resulted in the first global mapping of these space plasma regions -- the magnetosphere -- into the ionosphere of the Earth, under a variety of conditions. For example, Newell and Meng [1994] showed the dramatic effects solar wind pressure has on the mapping of plasma regions into the ionosphere.

The third step continuing in the same logical progression is the identification and monitoring of the magnetosphere through multiwavelength UV auroral imagery. However this requires calibrating the UV signatures to the particle specifications of the plasma source regions. It is fairly clear that the UV images contain the information needed for global monitoring of the magnetosphere in principle, but it is first necessary to develop a methodology for deconvolving the plasma distribution and behavior from the images. Some very preliminary efforts using Polar BEAR and DMSP satellites have already conducted [Newell *et al.*, 1992], but unfortunately Polar BEAR had only limited capabilities in terms of choosing the wavelengths that could be simultaneously monitored, and it is not possible to accurately determine the magnetosphere's plasma distribution with this satellite.

The future DMSP satellites will contain the SSUSI imager which will allow a more fruitful combination of wavelengths. In anticipation, Meng [1994] has carried out some of the preliminary analysis necessary to exploit the new data set, by converting the particle maps of plasma distributions [Newell and Meng, 1992] into intensities at various wavelengths.

In addition to the logical chain above, leading to the monitoring of the magnetosphere from global auroral imagery, a second promising path has emerged from work on the nightside precipitation. It turns out that in many ways the state of the magnetosphere can be more accurately determined from a careful study of nightside precipitation than anyone had supposed. The results of our research into this problem over the last 1.5 years are quite significant, and we now devote some space to explaining them.

Our investigation into systematizing nightside precipitation centered on extracting the features of greatest geophysical significance. The proposed system, which includes operational definitions and has been automated, consists of: boundary (b1) The "zero-energy" convection boundary (often the plasmopause); boundary (2e) The point where the large-scale gradient of electron average energy with latitude,  $dE_e/d\lambda$ , switches from positive to  $\leq 0$  (the start of the main plasma sheet); boundary (2i) The ion high-energy precipitation cutoff (the ion isotropy boundary or the start of the tail current sheet); boundary (3a,b) The most equatorward and poleward electron acceleration events

(spectra with "monoenergetic peaks") above  $0.25 \text{ ergs/cm}^2 \text{ s}$ ; boundary (4s) Transition of electron precipitation from unstructured on a  $\geq 10 \text{ km}$  spatial scale (spectra have 0.6-0.95 correlation coefficients with neighbors) to structured precipitation (correlation coefficient usually 0.4 and below); boundary (5) The poleward edge of the main auroral oval, marked by a spatially sharp dropoff in energy fluxes by a factor of at least 4 to levels below that typical of the auroral oval; boundary (6) The poleward edge of the subvisual drizzle often observed poleward of the auroral oval.

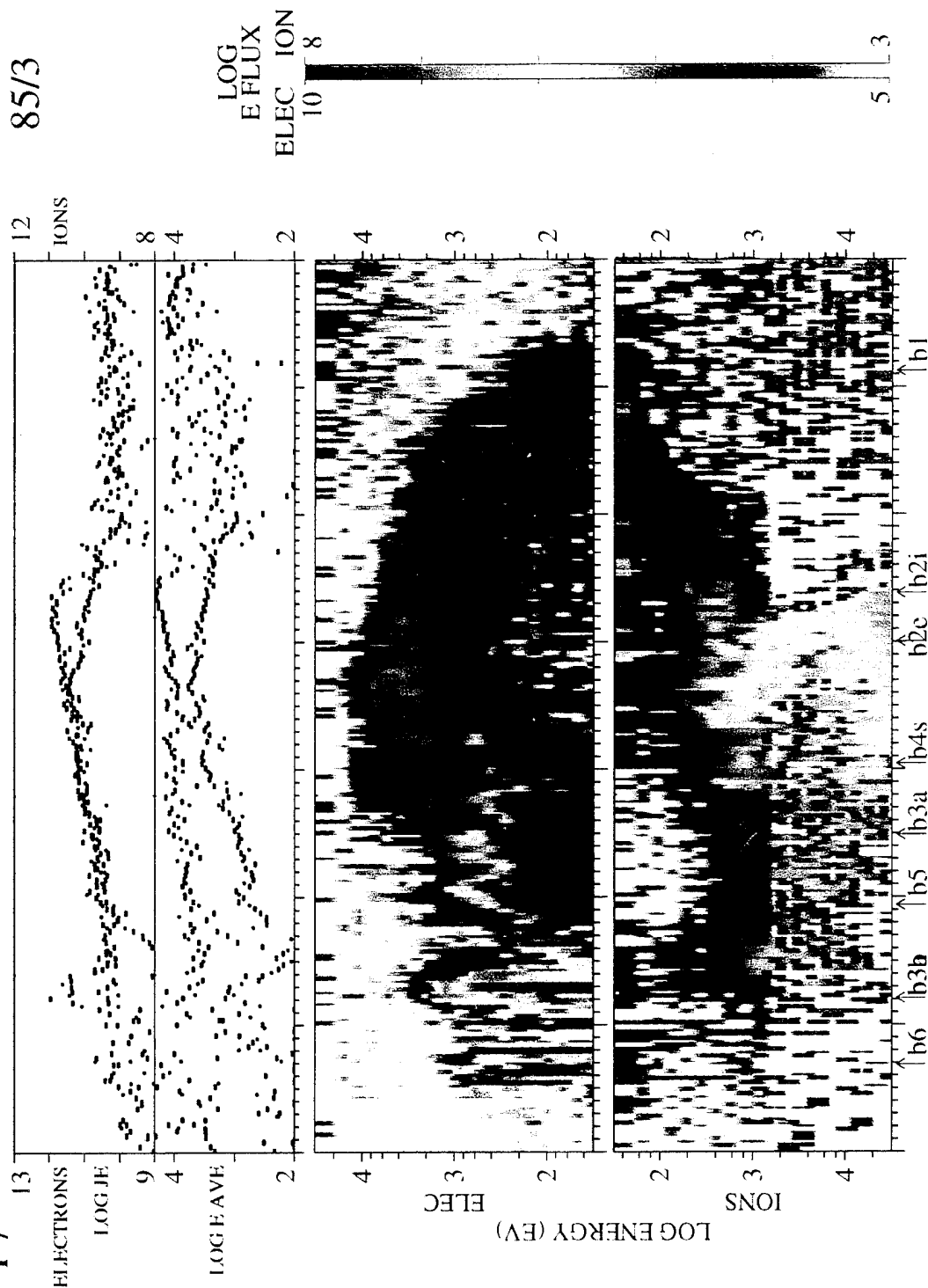
As has been mentioned, the boundaries were chosen so that they (1) contained as much geophysical significance as possible, and (2) were amenable to automated identification. What follows in section 2 is a more detailed explication of each boundary with respect to geophysical significance; in section 3 a brief summary of operational identifications will be given.

## 2. The Structure of Nightside Precipitation: Physical Significance of the Boundaries

As in many situations, an example is clearer than words alone; hence consider Figure 1, which presents a DMSP F7 pass at 11:23 UT on January 3, 1985. We consider in turn each of the most geophysically significant boundaries that can be identified in this picture. Because operational definitions which are robust require an attention to detail that is tedious to many, the present section gives conceptually oriented definitions, with the fine print reserved for Section 3.

(1) The "zero-energy" convection boundary (11:27:13 UT). Zero-energy electrons and ions have no curvature and gradient drifts, hence they should share a common equatorward boundary; one which is determined purely by the electric and magnetic field configuration. (That is, the boundary which results only from a consideration of  $\mathbf{ExB}$  drift effects). The DMSP low-energy ion detector has an extremely large geometric factor, which makes it possible to observe such coincidences despite the comparatively low fluxes of ions at low energies. Newell and Meng [1988b] have reported that in the dusk and midnight sectors the electron and ion zero energy cutoffs indeed coincide on 80% of the passes. To maintain operational unambiguity, we propose that the zero-energy electron and ion boundaries be separately defined (denoted b1e and b1i). Then, when the two boundaries indeed coincide to within  $0.25^\circ$  magnetic latitude, one may reasonably say that a zero-energy convection boundary exists. Any model electric and magnetic field of the magnetotail specifies a unique position for this boundary (as a function of MLT); hence observation of the boundary provides a direct comparison between theory and reality. In some theoretical formulations, the zero-energy convection boundary is also the plasmopause location [Nishida, 1966], and indeed observations of electron data support this association [Galperin et al., 1977; Horwitz et al., 1986; Sauvaud et al., 1983]. However the zero-energy boundary observed at any given time does not necessarily represent a steady-state convection boundary, since magnetotail convection is highly dynamic [Mauk and Meng, 1983]. Indeed, the low-energy equatorward ion precipitation often contains plasma originally of ionospheric origin, apparently injected at high latitudes often in association with auroral arcs [Bosqued et al., 1986]. However its subsequent convection towards lower latitudes is the result of  $\mathbf{ExB}$  drift effects. To maintain operational unambiguity, and because the zero-energy boundary has theoretical importance in its own right, we do not here stress the connection with the plasmopause.

F7



85/3

Jan 3

UT	11:23:30	11:24:04	11:24:38	11:25:12	11:25:46	11:26:20	11:26:54	11:27:29
MLAT	75.1	73.2	71.2	69.2	67.2	65.3	63.2	61.3
GLAT	76.5	75.0	73.3	71.6	69.8	68.0	66.1	64.2
GLONG	202.1	196.5	192.4	188.8	185.9	183.4	181.1	179.3
MLT	22:45	22:43	22:43	22:42	22:42	22:42	22:41	22:41

Figure 1

(2e) The poleward edge of the  $dE_e/d\lambda > 0$  region (11:25:47 UT). It has long been known that low-energy electrons in the plasma sheet reach closer to Earth than do higher energy electrons [Vasyliunas, 1968; Schield and Frank, 1970; Fairfield and Vinas, 1984]. The higher the energy of the electrons measured, the further from the Earth they appear to have a cutoff (some exceptions exist, such as when a dispersionless injection occurs). As a low-altitude spacecraft moves poleward from boundary 1e, progressively higher-energy electrons are observed; so  $dE_e/d\lambda > 0$  (where  $E_e$  is the e- average energy). As one reaches the main plasma sheet, electrons of all energies are observed. Further poleward the overall trend is for  $dE_e/d\lambda < 0$  (the region of negative gradient has a slope of smaller magnitude and exhibits more fluctuations than does the region of positive gradient). This is simply because the plasma sheet is progressively colder further from the Earth. The point where  $dE_e/d\lambda = 0$  is one measure of the start of the main plasma sheet -- or in the terminology of *Feldstein and Galperin* [1985] (hereinafter FG85) the true start of the central plasma sheet.

(2i) The high-energy ion equatorward precipitation cutoff (precipitating energy flux maximum -- 11:26:00 UT). This boundary is also the Isotropy Boundary (IB) of Sergeev et al. [1983]. It is probably the best and most direct proxy for the location of the Earthward edge of the current sheet. Consider ions in the energy range from a few keV to tens of keV (30 keV for DMSP). Ions in this energy range increase in temperature and energy flux with declining latitude, apparently as a result of adiabatic acceleration as plasma convects Earthward in the magnetotail [Galperin et al., 1977]. This steady temperature increase terminates with a relatively sharp equatorward precipitation cutoff. However in the high-altitude inner magnetosphere, ions do not disappear at the L-shell value of the high-energy ion precipitation boundary [e.g., Lui et al., 1987]. Instead what changes is that the ions become trapped, and cease to precipitate in measurable quantities. Poleward of the precipitation boundary at any particular energy, the ions are highly isotropic [Bernstein et al., 1974; Sergeev et al., 1993]. It has thus been suggested, and even successfully modeled in some detail, that the ions maintain their isotropy by pitch angle scattering in the tail current sheet [Lyons and Speiser,]. The physical mechanism is quite simple: ions cannot maintain pitch angle while bending around field lines which have a radius of curvature comparable to the ion gyroradii [Sergeev et al., 1983]. This explanation also accounts for the dispersion in the high-energy ion cutoffs [Sergeev et al., 1993]. The larger gyroradii of higher energy ions means that they scatter off field lines with smaller radii of curvature than do the lower energy ions; hence the higher-energy ions maintain isotropy further Earthward.

Neither the tail current sheet nor the precipitating high-energy ions have a sharply defined boundary. Operationally we propose to use the ion precipitating energy flux peak (integrated over the range 3 keV to 30 keV), which universally occurs close to the equatorward boundary of the high-energy ion precipitation, as the location of b2i. The geophysical significance of the boundary is that it represents a good approximation to the Earthward edge of the tail current sheet. Sergeev and Gvozdevsky [1995] have demonstrated that the latitude of this ion isotropy boundary has a very high correlation ( $r \sim 0.9$ ) with the magnetic field inclination (degree of stretching) measured simultaneously at the geomagnetic equator.

A boundary closely related conceptually is the  $> 30\text{-}40$  keV electron trapping boundary for electrons, which we term b2t. Although we cannot directly identify it in our DMSP data base, it has a long history of being considered useful. Thought in the 1960s to represent the open/closed field line boundary, b2t is now generally recognized as another measure of where field lines begin to be significantly stretched. Because of the smaller gyroradii of electrons, b2t usually lies a short distance poleward of b2i. There is some reason to believe that the stable trapping boundary approximately corresponds to the *Winningham et al.* [1975] (hereinafter WYAH75) boundary between CPS and BPS; and indeed Weiss et al. [1992] define this latter boundary by the trapping boundary.

(3a,b) The most equatorward and poleward e- acceleration events. In the literature many proxies for identifying the region of discrete auroras exist. For example it appears that most electron acceleration events, and certainly those of high accelerating potential values, occur on the stretched field lines that lie poleward of the  $> 40$  keV e- stable trapping boundary [Frank and Ackerson, 1971]. It is quite feasible to individually examine each electron spectrum and determine whether it shows signs of a field-aligned accelerating potential. Therefore we include boundaries 3a and 3b, which, based on the examination of each individual spectrum, are the furthest equatorward and furthest poleward sites of electron acceleration. A spectrum is identified as accelerated if it either has a monoenergetic peak, or a sharp cutoff above the spectral peak (more detail is available in Newell et al. [1996]). Although we have opinions about the likely location of these boundaries, it is best that they be identified separately from all other precipitation boundaries.

Boundary 4s-- the onset of spatial structure in electron precipitation (on a scale  $\geq 5\text{-}10$  km) (11:25:14). The BPS/CPS distinction, no matter what misconceptions became associated with it, has persisted primarily because many nightside crossings do seem to have a highly structured region and a relatively unstructured region of auroral electron precipitation. If this structured/unstructured distinction represents something fundamental, there should be a quantitative way of making the distinction within the precipitation data itself, i.e., one which does not depend on such additional factors such as the boundary of the radiation belts (b2t).

To move from a qualitative description ("structured") to a quantitative description, we investigated the behavior of the correlation coefficient of individual spectra with their neighbors. Figure 2 shows a plot of the running average of the correlation coefficient of each spectra in Figure 2 with the previous 5 spectra. (Our algorithm suppresses spectra with fluxes below  $0.25$  ergs/cm<sup>2</sup> s by halving the correlation coefficient.) Although even within the "BPS" region the majority of the individual spectra do not show evidence of field-aligned acceleration, Figure 2 shows that the entire region is indeed structured in the sense that each point correlates only poorly with its neighbors. We therefore introduce boundary 4s, the structured precipitation boundary, defined by the point where the correlation coefficient drops from the  $0.95\text{-}0.60$  range to below  $0.60$ . Thus b4s marks a fundamental change in the character of the electron precipitation, from a spatially unstructured region to a highly structured region.

Boundary 5(e,i) -- The poleward boundary of the main auroral oval (11:24:36 UT). The precipitating energy flux in the auroral oval typically drops by about an order of



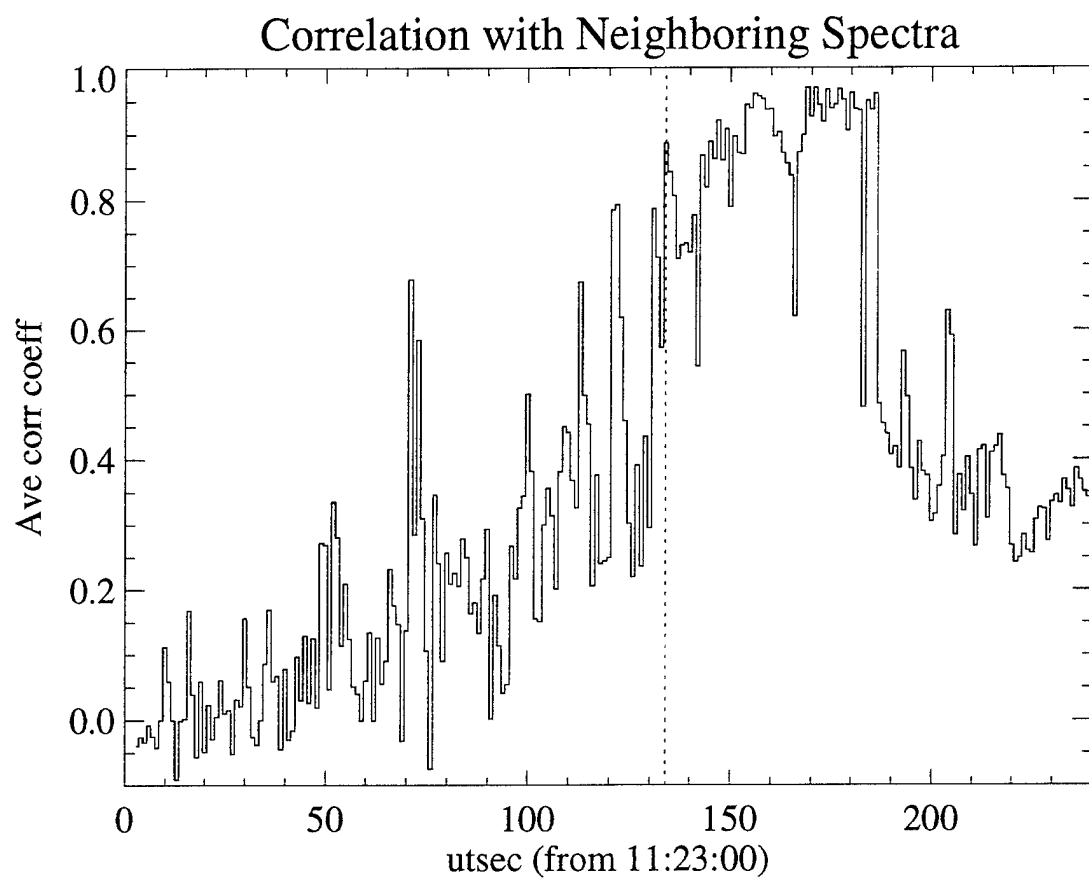


Figure 2

magnitude over a short distance (usually  $< \sim 0.20$ ). This dramatic dropoff occurs in both the electrons and ions, although not always in precisely the same location for the two species. In active times, poleward of this sharp dropoff there is often only a narrow region of high energy ( $\sim 10$  keV) but diffuse electrons at a very low flux levels. (This faint "overhang" of high-energy electrons seems to be both an unremarked feature in the literature and a common feature in nature). Sometimes, especially in quiet times, including quieting times following a substorm, a subvisual drizzle can extend poleward of the oval. The conceptual definition of the poleward edge of the main auroral oval is that the precipitating fluxes drop by a factor of at least 4 over a short distance to values below  $3 \times 10^{10}$  eV/cm<sup>2</sup> s str (e-) or  $10^{10}$  eV/cm<sup>2</sup> s str (ions). We emphasize that even for northward IMF conditions such sharp dropoffs still occur, and separate the main auroral oval from the polar cap precipitation (which, to be sure, usually resembles the structured plasma sheet precipitation although not at the intensity of the main oval).

Boundary 6. The poleward boundary of the subvisual drizzle (11:23:53 UT). Poleward of the main auroral oval is a weak subvisual drizzle that differs from polar rain in several ways. The subvisual drizzle usually includes weak ion as well as electron precipitation; the drizzle is structured, while polar rain is comparatively homogeneous; and the typical electron energies are a bit higher than normal for polar rain. Polar rain is intense poleward of the dayside oval, and declines gradually in intensity moving towards the nightside oval. The subvisual drizzle extends poleward from the nightside oval and terminates either when fluxes drop to background levels, or (less commonly) when a smooth coherent electron polar rain signature is encountered.

### 3. Operational Definitions of Nightside Precipitation

In this section we give the (sometimes tedious) detail required to operationally define the various boundaries unambiguously. The integral parameters are denoted  $n$ ,  $jE$ , and  $E$ , referring to density, energy flux, and average energy respectively. These quantities can be subscripted by "e" and "i" for electrons and ions. Better results are obtained if the terms  $jep(E1,E2)$  etc are introduced, referring to the "partial" electron energy flux between  $E1$  and  $E2$ . Strictly speaking all instruments measure only a partial values of "integral" parameters between the upper and lower ranges of their detector (some confusion in the literature exists from the neglect of this point, as in the case of the cusp electron average energy). As a practical consideration here, such partials improve greatly the identification of boundaries while also making the results somewhat less dependent on the specific detector (SSJ4) that they were designed for. The units used below are eV for  $E$ , and  $\log_{10}$  eV/cm<sup>2</sup> s str for  $jep$ ,  $jip$ .

For each boundary, we start by giving the rule which works most of the time, and follow with caveats and more detail on handling special cases.

--  $b1e,i$  (zero-energy). The algorithm moves from lower latitudes to higher, comparing the average of  $jip(E1,E2)$  and  $jep(E1,E2)$  (ordinarily  $E1$  and  $E2$  are the 2 lowest channels) over the 3 previous spectra with the 3 succeeding spectra. An increase in  $jip$  by a factor of 2 marks the onset of the zero energy boundary, which is separately determined for the two species. This jump is significant only if it also significantly exceeds the background counts gotten by averaging over several equatorward seconds. If  $jep$  rises to a value above 8.0 ( $jip$  reaches 6.5) a factor of only 1.6 jump is acceptable in determining

the zero-energy boundary. If  $j_{ep} > 8.25$  ( $j_{ip} > 6.9$ ), it is assumed that the boundary has been reached, even if no jump in the value of the fluxes is measured.

Special cases: The energy range considered ( $E1$  to  $E2$ ) in the partials depends on whether photoelectrons are present, and whether the spacecraft is charged to  $-28$  V. The former can be identified by a sharp dropoff in electron fluxes above  $68$  eV at latitudes below the auroral zone; the latter by a sharp cutoff above the  $32$  eV ion channel. In the absence of these effects, the channels are set to the lowest available,  $E1=32$ ,  $E2=47$ . If the spacecraft is charged to  $-28$  V, the ion channels are set to  $E1=47$ ,  $E2=68$ . If photoelectrons are present (rare on the nightside), the next available "clean" channels are  $100$  and  $145$  eV. Finally sometimes isolated noise can cause false positives, as by radiation belts counts. Thus a "checkb1e" routine performs a double check by simply examining the next several seconds. If instead of rising fluxes as the auroral oval is entered, the next few seconds exhibit a dropoff in fluxes, the identification of b1e is inaccurate and the search resumes towards increasing latitudes.

--- b2e (plasma sheet start). This algorithm locates the first point poleward of b1e where  $dE_e/dl \leq 0$ . A sliding 3-s average  $E_e$  is compared to that of any three consecutive seconds over the next 9 s. If the value of  $E_e$  does not rise over this interval, the boundary b2e has been located.

Special cases: If the correct boundary b2e has been found, one expects to have entered the main plasma sheet. Hence if  $j_{Ee} < 11$  (or if both  $j_{Ee} < 11.5$  and  $E_e < 1000$  eV) then the next 30 seconds are examined, to see if a spectra exists with both higher  $E_e$  and a  $j_e$  larger by at least  $0.3$  (i.e., a factor of 2 difference in the energy flux). This double checking is done only under these suspicious circumstances of low fluxes, because it risks encountering a point with high  $E_e$  and high  $j_e$  simply because strong field-aligned acceleration is encountered.

--b2i (ion isotropy boundary). This boundary is defined by the precipitation flux maxima for ions  $3$  keV and above. The high-energy ions behave less variably than do the electrons, so fewer precautions are needed. Thus a sliding average of  $j_{ip}(3 \text{ keV}, 30 \text{ keV})$  over 2 seconds is compared to  $j_{ip}$  for any three consecutive seconds over the next 10 s further poleward to determine whether the maxima has been located. The smallest maxima acceptable is  $10.5$ .

Special cases: Sometimes "nose" events occur, namely the injection of high energy ion regions slightly detached from the rest of the auroral oval [Konradi et al., 1975; Sánchez et al., 1993]. Such events are identified as a local maxima followed by a decline and subsequent rise to a global energy flux maxima. The detached (or partially detached) maxima is discarded.

Additional Note: It is possible (in times of prolonged quiet) for b2i to occur equatorward of b1i; but by definition b2e must always lie poleward of b1e.

--b3a,b (most equatorward and poleward e- acceleration events). Each individual spectra is examined for evidence of a monoenergetic peak. This can either be a single channel with a differential energy flux 5 times larger than any other; or a sharp drop by at least a factor of 10 below the electron differential energy flux peak. Details on this algorithm, including special cases, are presented in a separate paper [Newell et al., 1996]. The most equatorward and poleward individual spectra showing such "monoenergetic" peaks are flagged as boundaries b3a and b3b, without regard to the other boundary locations.

--b4s (structured/unstructured boundary). The counts in the various channels for a given spectrum are correlated with the corresponding counts in the 5 previous spectra, and the 5 resulting correlation coefficients are averaged ( $\langle r \rangle$ ). By definition b4s lies poleward of b2e and b2i. When the sum of seven consecutive  $\langle r \rangle$  drops below 4.0, the search is halted. b4s is set to be the furthest poleward spectra within the current group of 7 seconds which has  $\langle r \rangle > 0.60$ .

Special cases: If the energy fluxes result only in an aurora which is subvisual ( $j_e < 10.7$ , or  $0.25 \text{ ergs/cm}^2 \text{ s}$ ) the correlation coefficient is suppressed (halved); hence low flux but homogeneous regions such as polar rain are automatically excluded.

---b5e,b5i (poleward edge of main oval). The boundaries are computed separately, but using the same procedure. An average of  $jE$  for the previous 12 seconds is compared with  $jE$  for the succeeding 12 seconds. When a dropoff of a factor of 4 is located, a provisional b5 boundary is determined. Note that this algorithm emphasizes locating a sharp drop in the flux levels.

Special cases. The next 30 s are double checked (35 s for e-) to make sure the dropoff remained below auroral energy fluxes. If the (log) average  $jE$  has not dropped below about 9.7 for ions or 10.5 for electrons, the search continues for the corresponding b5 boundary. Such a large search ahead is needed because of features such as the "double oval" [Elphinstone et al., 1995] in which fluxes temporarily drop below oval levels only to rise again clearly to oval values.

---b6. The poleward boundary of the subvisual drizzle is defined by the point where either polar rain is encountered (identified by the presence of unstructured electrons and no ions) or  $j_e$  drops below 10.4 and  $j_i$  drops below 9.6.

Special cases: The drizzle is defined by weak structured fluxes with ions and electrons above noise levels. By checking the computed average energy one can infer whether noise is significant: For example if counts are randomly distributed across all channels one would obtain  $E = 15 \text{ keV}$  for DMSP. If  $E_e < 500 \text{ eV}$ , even a flux as low as 10.0 is acceptable. The lower the average energy the lower a flux level is acceptable as not representing noise.

#### 4. Summary

The major progress made within the 4 year cycle (including the year under a no-cost extension) of AFOSR grant F49620-92-J-0196 occurred in two major areas. The first is a further development of the research line originating in our multi-year effort to identify the source region of dayside precipitation regions as accurately as possible. Because the ionosphere is a much more compact and cheaply accessible region to sample than is the magnetosphere to which it is geomagnetically connected, the benefits of this approach to investigating and monitoring the state of the magnetosphere are manifold.

Major research accomplishments along this line of endeavor include creating maps of the ionosphere's connection to the magnetosphere under varying conditions of solar wind pressure [Newell and Meng, 1994]. Since the logical extension of this work for monitoring the magnetosphere includes the identification of magnetospheric boundaries from multi-spectral imagery, some preliminary feasibility work in this direction has been carried out [Newell et al., 1992; Meng, 1994].

Because much of magnetospheric dynamics, and in particular large magnetic storms affecting Air Force operational environments, occurs on the nightside, we have within

the last grant cycle considered the problem of monitoring of the state of the magnetosphere from nightside precipitation structure. The boundaries of greatest geophysical significance were identified, and automated algorithms created and tested for their identification. Although our system of dayside identifications has had considerable academic impact, being both widely cited and widely incorporated by other researchers into their investigations of the magnetosphere from ground based and low-altitude measurements, it has not directly led to any immediate improvements in space weather forecasting. Our new work, completed in the latest grant cycle and discussed in sections 2 and 3 of the present report, extends the sophisticated monitoring of the magnetosphere into the dynamic region of the nightside. We expect that the impact on other researchers of the near-Earth space system will be comparable to that of the dayside work; moreover we believe that the new system will be more likely to direct lead to improvements in space weather forecasting.

## References

- Bernstein, W., B. Hultqvist, and H. Borg, Some implications of low altitude observations of isotropic precipitation of ring current protons beyond the plasmapause, *Planet. Space Sci.*, 22, 767, 1974.
- Bosqued, J. M., J. A. Sauvaud, and D. Delcourt, Precipitation of superthermal ionospheric ions accelerated in the conjugate hemisphere, *J. Geophys. Res.*, 91, 7006, 1985.
- Cambou, F., and Yu. I. Galperin, Overall results from the ARCAD experiment aboard the satellite AUREOLE paper M7-8, in *International Symposium on Solar-Terrestrial Physics*, Sao Paulo, p. 396, Brazil, 1974.
- Cambou, F., and Yu. I. Galperin, Main results of the joint French-Soviet space project ARCAD-1 and ARCAD-2 for magnetospheric, auroral and ionospheric physics, *Annales de Geophysique*, 38, 87, 1982.
- Eather, R. H., Latitudinal distributions of auroral and airglow emissions: The "soft" auroral zone, *J. Geophys. Res.*, 74, 153, 1969.
- Elphinstone, R. D., J. S. Murphree, D. J. Hearn, L. L. Cogger, I. Sandahl, P. T. Newell, D. M. Klumpar, S. Ohtani, J. A. Sauvaud, T. A. Potemra, K. Mursula, A. Wright, and M. Shapshak, The double oval UV auroral distribution: 1. Implications for the mapping of auroral arcs, *J. Geophys. Res.*, 100, 12075, 1995.
- Feldstein, Y. I., and Yu. I. Galperin, The auroral luminosity structure in the high-latitude upper atmosphere: Its dynamics and relationship to the large-scale structure of the Earth's magnetosphere, *Rev. Geophys.*, 23, 217, 1985.
- Frank, L. A., and K. L. Ackerson, Observations of charged particle precipitation into the auroral zone, *J. Geophys. Res.*, 76, 3612, 1971.
- Galperin, Yu. I., and Ya. I. Feldstein, Auroral luminosity and its relationship to magnetospheric plasma domains, in *Auroral Physics*, edited by C.-I. Meng, M. J. Rycroft, and L. A. Frank, Cambridge Univ. Press, p. 207, 1991.
- Galperin, Yu. I., N. V. Jorjio, R. A. Kovrazhkin, F. Cambou, J. A. Sauvaud, J. Crasnier, On the origin of auroral protons at the day-side auroral oval, *Ann. Geophys.*, 32, 117, 1976.
- Galperin, Yu. I., V. A. Gladyshev, N. V. Jorjio, R. A. Kovrazhkin, V. M. Sinitsin, F. Cambou, J. A. Sauvaud, and J. Crasnier, Adiabatic acceleration induced by convection in the plasma sheet, *J. Geophys. Res.*, 83, 2567, 1978.
- Horwitz, J. L., S. Menteer, J. Turnley, J. L. Burch, J. D. Winningham, C. R. Chappell, J. D. Craven, L. A. Frank, and D. W. Slater, Plasma boundaries in the inner magnetosphere, *J. Geophys. Res.*, 91, 8861, 1986.
- Konradi, A., C. L. Semar, and T. A. Fritz, Substorm-injected protons and electrons and the injection boundary model, *J. Geophys. Res.*, 80, 3055, 1975.
- Lassen, K., J. R. Sharber, and J. D. Winningham, The development of auroral and geomagnetic substorm activity after a southward turning of the interplanetary magnetic field following several hours of magnetic calm, *J. Geophys. Res.*, 82, 5031, 1977.
- Lui, A. T. Y., R. W. McEntire, and S. M. Krimigis, Evolution of the ring current during two geomagnetic storms, *J. Geophys. Res.*, 92, 7459, 1987.

- Lyons, L. R., Generation of large-scale regions of auroral currents, electric field potentials, and precipitation by the divergence of the convection electric field, *J. Geophys. Res.*, 85, 17, 1980.
- Lyons, L. R., and T. W. Speiser, Evidence for current sheet acceleration in the geomagnetic tail, *J. Geophys. Res.*, 87, 2276, 1982.
- Lyons, L. R., and J. C. Samson, Formation of the stable auroral arc that intensifies at substorm onset, *Geophys. Res. Lett.*, 19, 2171, 1992.
- Lyons, L. R., J. F. Fennell, and A. L. Vampola, A general association between discrete auroras and ion precipitation from the tail, *J. Geophys. Res.*, 93, 12932, 1988.
- Meng, C.-I., Space borne optical remote sensing of midday auroral oval and different precipitation regions, in *Physical Signatures of Magnetospheric Boundary Layer Processes*, ed. Jan Holtet and Alv Egeland, p. 157, Kluwer Academic Publishers, Dordrecht, 1994.
- Newell, P. T., and C.-I. Meng, Energy dependence of the equatorward cutoffs in auroral electron and ion precipitation, *J. Geophys. Res.*, 92, 7519, 1987.
- Newell, P. T., and C.-I. Meng, The cusp and the cleft/boundary layer: Low altitude identification and statistical local time variation, *J. Geophys. Res.*, 93, 14549, 1988a.
- Newell, P. T., and C.-I. Meng, Categorization of dispersion curves in the equatorward edge of the diffuse aurora, *Planet. Space Sci.*, 36, 1031, 1988b.
- Newell, P. T., W. J. Burke, C.-I. Meng, E. R. Sánchez, and M. E. Greenspan, Identification of the plasma mantle at low altitude, *J. Geophys. Res.*, 96, 35, 1991a.
- Newell, P. T., W. J. Burke, E. R. Sánchez, C.-I. Meng, M. E. Greenspan, and C. R. Clauer, The low-altitude boundary layer and the boundary plasma sheet at low-altitude: Prenoon precipitation regions and convection reversal boundaries, *J. Geophys. Res.*, 96, 21013, 1991b.
- Newell, P. T., S. Wing, C.-I. Meng, and V. Sigillito, The auroral oval position, structure, and intensity of precipitation from 1984 onward: an automated online data base, *J. Geophys. Res.*, 96, 5877, 1991c.
- Newell, P. T., C.-I. Meng, and R. E. Huffman, Determining the source region of auroral emissions in the prenoon oval using coordinated Polar BEAR UV-imaging and DMSP particle measurements, *J. Geophys. Res.*, 97, 12245, 1992.
- Newell, P. T., K. M. Lyons, and C.-I. Meng, A large survey of electron acceleration events, (in press) *J. Geophys. Res.*, 1995.
- Newell, P. T., Y. I. Feldstein, Y. I. Galperin, and C.-I. Meng, The morphology of nightside precipitation, (in press), *J. Geophys. Res.*, 1995.
- Nishida, A., Formation of plasmopause, or magnetospheric plasma knee, by the combined action of magnetosphere convection and plasma escape from the tail, *J. Geophys. Res.*, 71, 5669, 1966.
- Sánchez, E. R., B. H. Mauk, P. T. Newell, and C.-I. Meng, Low-altitude observations of the evolution of substorm injection boundaries, *J. Geophys. Res.*, 98, 5815, 1993.
- Sauvaud, J. A., Yu. I. Galperin, V. A. Gladyshev, A. K. Kuzmin, T. M. Muliarchick, and J. Crasnier, Spatial inhomogeneity of magnetosheath proton precipitation along the dayside cusp from the Arcad experiment, *J. Geophys. Res.*, 85, 5105, 1980.
- Sauvaud, J. A., J. Crasnier, K. Moula, R. A. Kovrazhkin, and N. V. Jorjio, Morning sector ion precipitation following substorm injections, *J. Geophys. Res.*, 86, 3430, 1981.

- Sauvad, J. A., J. Crasnier, Yu. I. Galperin, and Y. I. Feldstein, A statistical study of the dynamics of the equatorial boundary of the diffuse aurora in the pre-midnight sector, *Geophys. Res. Lett.*, 10, 749, 1983.
- Senior, C., D. C. Delcourt, J. C. Cerisier, C. Hanuise, J. P. Villain, R. G. Greenwald, P. T. Newell, F. J. Rich, Correlated observations of the boundary between polar cap and nightside auroral zone by HF radars and the DMSP satellite, *Geophys. Res. Lett.*, 21, 221, 1994.
- Sergeev, V. A., E. M. Sazhina, N. A. Tsyganenko, J. A. Lundblad, and F. Soraas, Pitch-angle scattering of energetic protons in the magnetotail current sheet as the dominant source of their isotropic precipitation into the nightside ionosphere, *Planet. Space Sci.*, 31, 1147, 1983.
- Sergeev, V. A., M. Malkov, and K. Mursula, Testing the isotropic boundary algorithm method to evaluate the magnetic field configuration in the tail, *J. Geophys. Res.*, 98, 7609, 1993.
- Sergeev, V. A., and B. B. Gvozdevsky, MT-index -- a possible new index to characterize magnetic configuration of magnetotail, *Ann. Geophys.*, (in press), 1995.
- Schild, M. A., and L. A. Frank, Electron observations between the inner edge of the plasma sheet and the plasmasphere, *J. Geophys. Res.*, 75, 5401, 1970.
- Vasyliunas, V. M., A survey of low-energy electrons in the evening sector of the magnetosphere with OGO 1 and OGO 3, *J. Geophys. Res.*, 73, 2839, 1968.
- Weiss, L. A., P. H. Reiff, R. V. Hilmer, J. D. Winningham, and G. Lu, Mapping the auroral oval into the magnetotail using Dynamics Explorer plasma data, *J. Geomag. Geoelectr.*, 44, 1121, 1992.
- Winningham, J. D., F. Yasuhara, S.-I. Akasofu, and W. J. Heikkila, The latitudinal morphology of 10-eV to 10-keV electron fluxes during magnetically quiet and disturbed times in the 2100-0300 MLT sector, *J. Geophys. Res.*, 80, 3148, 1975.
- Zelenyi, L., R. Kovrazkhin, and J.-M. Bosqued, Velocity dispersed ion beams in the nightside auroral zone: Aureol-3 observations, *J. Geophys. Res.*, 95, 12119, 1990.



## II. TECHNICAL INFORMATION: AFOSR GRANT F49620-92-J-0196    Supported Publications (1992-1995) in Refereed Journals

1. Anderson, H. M., M. J. Engebretson, R. L. Arnoldy, L. J. Cahill, and P. T. Newell, Statistical study of hydromagnetic chorus events at very high latitudes, *J. Geophys. Res.*, 100, 3681, 1995.
2. Baker, K. B., J. R. Dudeney, R. A. Greenwald, M. Pinnock, P. T. Newell, A. S. Rodger, N. Mattin, and C.-I. Meng, HF-radar signatures of the cusp and low latitude boundary layer, *J. Geophys. Res.*, 100, 7671, 1995.
3. Burke, W. J., B. Jacobsen, P. E. Sandholt, W. F. Denig, N. C. Maynard, and P. T. Newell, Optical signatures and sources of prenoon auroral precipitation, *J. Geophys. Res.*, 98, 11521, 1993.
4. Cumnock, J. A., R. A. Heelis, M. R. Hairston, and P. T. Newell, High-latitude ionospheric convection pattern during steady northward interplanetary magnetic field, 14537, 1995.
5. de la Beaujardiere, O., L. R. Lyons, J. M. Ruohoniemi, E. Friis-Christensen, C. Danielsen, F. J. Rich, and P. T. Newell, Quiet-time intensifications along the poleward auroral boundary near midnight, *J. Geophys. Res.*, 99, 287, 1994.
6. de la Beaujardiere, O., J. Watermann, P. Newell, and F. Rich, Relationship between Birkeland current regions, particle precipitation, and electric fields, *J. Geophys. Res.*, 98, 7711, 1993.
7. Elphinstone, R. D., J. S. Murphree, D. J. Hearn, L. L. Cogger, P. T. Newell, and H. Vo, Viking observations of the UV dayside aurora and their relationship to DMSP particle boundary definitions, *Annales Geophysicae*, 10, 815, 1992.
8. Elphinstone, R. D., D. J. Hearn, L. L. Cogger, J. S. Murphree, H. Singer, V. Sergeev, K. Mursula, D. M. Klumpar, G. D. Reeves, M. Johnson, S. Ohtani, T. A. Potemra, I. Sandahl, E. Nielsen, M. Persson, H. Opgenoorth, P. T. Newell, and Y. I. Feldstein, Observations in the vicinity of substorm onset: Implications for the substorm process, *J. Geophys. Res.*, 100, 7937, 1995.
9. Elphinstone, R. D., J. S. Murphree, D. J. Hearn, L. L. Cogger, I. Sandahl, P. T. Newell, D. M. Klumpar, S. Ohtani, J. A. Sauvaud, T. A. Potemra, K. Mursula, A. Wright, and M. Shapshak, The double oval UV auroral distribution, 1, Implications for the mapping of auroral arcs, *J. Geophys. Res.*, 100, 12075, 1995.
10. Elphinstone, R. D., D. J. Hearn, L. L. Cogger, J. S. Murphree, A. Wright, I. Sandahl, S. Ohtani, P. T. Newell, D. M. Klumpar, M. Shapshak, T. A. Potemra, K. Mursula, and J. A. Sauvaud, The double oval UV auroral distribution: 2. The most poleward system and the dynamics of the magnetotail, *J. Geophys. Res.*, 100, 12093, 1995.
11. Feldstein, Y. I., P. T. Newell, S. V. Leontjev, V. G. Vorobjev, I. Sandahl, and J. Woch, Structure of auroral precipitation during a theta-aurora from multi-satellite observations, *J. Geophys. Res.*, 100, 17429, 1995.
12. Hansen, H. J., B. J. Fraser, F. W. Menk, Y. D. Hu, P. T. Newell, C.-I. Meng and R. J. Morris, High latitude Pc1 bursts originating within the low latitude boundary layer, *J. Geophys. Res.*, 97, 3993, 1992.

13. Hones, E. W., M. F. Thomsen, G. D. Reeves, D. J. McComas, and P. T. Newell, Observational determination of magnetic connectivity of the geosynchronous region of the magnetosphere to the auroral oval, (in press) *J. Geophys. Res.*, 1994.
14. Kan, J. R., C. S. Deehr, L. H. Lyu, and P. T. Newell, Ionospheric signatures of patchy-intermittent reconnection at dayside magnetopause, submitted to *J. Geophys. Res.*, 1995.
15. Lu, G., L. R. Lyons, P. H. Reiff, W. F. Denig, O. de la Beaujardiere, H. W. Kroehl, P. T. Newell, F. J. Rich, H. Opgenoorth, M. A. L. Persson, J. M. Ruohoniemi, E. Friis-Christensen, L. Tomlinson, R. Morris, G. Burns, and A. McEwin, Characteristics of ionospheric convection and field-aligned current in the dayside cusp region, *J. Geophys. Res.*, 100, 11845, 1995.
16. Lui, A. T. Y., R. D. Elphinstone, J. S. Murphree, M. G. Henderson, H. B. Vo, L. L. Cogger, H. Lühr, S. Ohtani, P. T. Newell, and G. D. Reeves, Special features of a substorm during high solar wind dynamic pressure, *J. Geophys. Res.*, 100, 19095, 1995.
17. Lopez, R. E., H. E. Spence, and C.-I. Meng, Substorm aurorae and their connection to the inner magnetosphere, *J. Geomag. Geoelectr.* 44, 1251, 1992.
18. Mauk, B. H., and C. E. McIlwain, Magnetic field-aligned electrodynamics of Alfvén/ion cyclotron waves, *J. Geophys. Res.*, 98, 19345, 1993.
19. McHarg, M. G., J. V. Olson, and P. T. Newell, ULF cusp pulsations: diurnal variations and interplanetary magnetic field correlations with ground based observations, *J. Geophys. Res.*, 100, 19729, 1995.
20. Meng, C.-I., Space borne optical remote sensing of midday auroral oval and different precipitation regions, *Physical Signatures of Magnetospheric Boundary Layer Processes*, 157, J. Holtet and A. Egeland, Editors, Kluwer Academic Publishers, Dordrecht, 1994.
21. Menk, F. W., B. J. Fraser, H. J. Hansen, P. T. Newell, C.-I. Meng, and R. J. Morris, Identification of the magnetospheric cusp and cleft using Pc1-Pc2 ULF pulsations, *J. Atmos. Terr. Phys.*, 54, 1021, 1992.
22. Minow, J., I., R. W. Smith, W. F. Denig, and P. T. Newell, Dayside auroral dynamics during reconfiguration of the auroral oval, *Physical Signatures of Magnetospheric Boundary Layer Processes*, 201, J. Holtet and A. Egeland, Editors, Kluwer Academic Publishers, Dordrecht, 1994.
23. Newell, P. T., W. J. Burke, E. R. Sánchez, C.-I. Meng, M. E. Greenspan, and C. R. Clauer, The LLBL and the BPS at low altitude: dayside precipitation regions and convection reversal boundaries, *J. Geophys. Res.*, 96, 21013, 1992.
24. Newell, P. T., C.-I. Meng, and R. E. Huffman, Determining the source region of auroral emissions in the pre-noon oval using coordinated Polar BEAR UV-imaging and DMSP particle measurements, *J. Geophys. Res.*, 97, 12245, 1992.
25. Newell, P. T., and C.-I. Meng, Mapping the dayside ionosphere to the magnetosphere according to particle precipitation characteristics, *Geophys. Res. Lett.*, 19, 609, 1992.
26. Newell, P. T., and C.-I. Meng, Reply, *Geophys. Res. Lett.*, 20, 1741, 1993.
27. Newell, P. T., and D. G. Sibeck,  $B_y$  Fluctuations in the Magnetosheath and Azimuthal Flow Velocity Transients in the Dayside Ionosphere, *Geophys. Res. Lett.*, 20, 1719, 1993.

28. Newell, P. T., and D. G. Sibeck, Upper limits on the contribution of Flux Transfer Events to ionospheric convection, *Geophys. Res. Lett.*, 20, 2829, 1993.
29. Newell, P. T., and C.-I. Meng, Ionospheric projections of magnetospheric regions under high and low solar wind pressure conditions, *J. Geophys. Res.*, 99, 273, 1994.
30. Newell, P. T., and D. G. Sibeck, Reply to Lockwood, Cowley, and Smith, *Geophys. Res. Lett.*, 21, 1821, 1994.
31. Newell, P. T., and C.-I. Meng, Comment on "Unexpected features of the ion precipitation in the so-called cleft/low latitude boundary layer: association with sunward convection and occurrence on open field lines" by Nishida, Mukai, Hayakawa, Matsuoka, Tsuruda, Kaya, and Fukunishi, *J. Geophys. Res.*, 99, 19609, 1994.
32. Newell, P. T., and D. G. Sibeck, Magnetosheath fluctuations and dayside ionospheric transients, *Physical Signatures of Magnetospheric Boundary Layer Processes*, 245, J. Holtet and A. Egeland Editors, Kluwer Academic Publishers, Dordrecht, 1994.
33. Newell, P. T., Do the dayside cusps blink?, *Rev. Geophys. Supplement, U.S. National Report to the IUGG (1991-1994)*, 665, 1995.
34. Newell, P. T., D. G. Sibeck, and C.-I. Meng, Penetration of the interplanetary magnetic field  $B_y$  and magnetosheath plasma into the magnetosphere: Implication for the predominant site of merging, *J. Geophys. Res.*, 100, 235, 1995.
35. Newell, P. T., and C.-I. Meng, Magnetopause dynamics as inferred from plasma observations on low-altitude satellites, *Physics of the Magnetopause*, P. Song and B. U. O. Sonnerup Editors, AGU Monograph 90, 407, 1995.
36. Newell, P. T., Y. I. Feldstein, Yu. I. Galperin, and C.-I. Meng, The morphology of nightside precipitation, (in press) *J. Geophys. Res.*, 1995.
37. Newell, P. T., and C.-I. Meng, Creation of theta-auroras: The isolation of plasma sheet fragments in the polar cap, *Science*, 270, 1338, 1995.
38. Newell, P. T., and C.-I. Meng, Cusp low-energy ion cutoffs: A survey and implications for merging, *J. Geophys. Res.*, 100, 21943, 1995.
39. Newell, P. T., K. M. Lyons, and C.-I. Meng, A large survey of electron acceleration events, (in press) *J. Geophys. Res.*, 1995.
40. Newell, P. T., and D. G. Sibeck, Transient versus quasi-steady merging: which describes the important physics?, submitted to *Eos* (invited debate), 1995.
41. Ohtani, S., B. J. Anderson, D. G. Sibeck, P. T. Newell, K. Takahashi, L. J. Zanetti, T. A. Potemra, R. E. Lopez, V. Angelopoulos, R. Nakamura, D. M. Klumpp, and C. T. Russell, A multisatellite study of a pseudo substorm onset in the near-Earth magnetotail, *J. Geophys. Res.*, 98, 19355, 1993.
42. Ohtani, S., T. A. Potemra, P. T. Newell, L. J. Zanetti, T. Iijima, M. Watanabe, M. Yamauchi, R. D. Elphinstone, O. de la Beaujardière, and L. G. Blomberg, Simultaneous Prenoon and postnoon observations of three field-aligned current systems from Viking and DMSP-F7, *Geophys. Res.*, 100, 119, 1995.
43. Ohtani, S., T. A. Potemra, P. T. Newell, L. J. Zanetti, T. Iijima, M. Watanabe, L. G. Blomberg, R. D. Elphinstone, J. S. Murphree, M. Yamauchi, and J. G. Woch, Four large-scale field-aligned current systems in the dayside high-latitude region, *J. Geophys. Res.*, 100, 137, 1995.

44. Ohtani, S., L. G. Blomberg, P. T. Newell, M. Yamauchi, T. A. Potemra, and L. J. Zanetti, Altitudinal comparison of dayside field-aligned current signatures by Viking and DMSP-F7: intermediate-scale FAC systems, submitted to *J. Geophys. Res.*, 1995.
45. Pinnock, M., A. S. Rodger, J. R. Dudeney, K. B. Baker, P. T. Newell, R. A. Greenwald, and M. E. Greenspan, Observations of an enhanced convection channel in the cusp ionosphere, *J. Geophys. Res.*, 98, 3767, 1993.
46. Ross, M., A. Christensen, C.-I. Meng, and J. Carbary, Structure in the UV nightglow observed from low Earth orbit, *Geophys. Res. Lett.*, 19, 958, 1992.
47. Samson, J. C., L. R. Lyons, P. T. Newell, F. Creutzberg, B. Xu, Proton aurora and substorm intensifications, *Geophys. Res. Lett.*, 19, 2167, 1992.
48. Sánchez, E. R., B. H. Mauk, P. T. Newell, and C.-I. Meng, Low-altitude observations of the evolution of substorm injection boundaries, *J. Geophys. Res.*, 98, 5815, 1993.
49. Sánchez, E. R., B. H. Mauk, and C.-I. Meng, Adiabatic vs. Non-adiabatic particle distributions during convection surges, *Geophys. Res. Lett.*, 20, 177, 1993.
50. Sánchez, E. R., J. M. Ruohoniemi, C.-I. Meng, and E. Friis-Christensen, Towards an observational synthesis of the substorm models: I: Poleward flows and high-latitude convection reversals observed in the nightside oval by PACE radars and DMSP satellites, submitted to *J. Geophys. Res.*, 1995.
51. Sibeck, D. G., and P. T. Newell, Concerning the location of magnetopause merging, *Physical Signatures of Magnetospheric Boundary Layer Processes*, J. Holtet and A. Egeland editors, 263-273, Kluwer Academic Publishers, Dordrecht, 1994.
52. Sibeck, D. G., and P. T. Newell, Interplanetary magnetic field orientation for transient events in the outer magnetosphere, *J. Geophys. Res.*, 100, 175-183, 1995.
53. Sibeck, D. G., and P. T. Newell, Pressure-pulse driven surface waves at the magnetopause: A rebuttal, *J. Geophys. Res.*, 100, 21773, 1995.
54. Sandholt, P. E., and P. T. Newell, A transient auroral event in the prenoon cusp-cleft ionosphere: ground and satellite observations, *J. Geophys. Res.*, 97, 8685, 1992.
55. Senior, C., D. C. Delcourt, J. C. Cerisier, C. Hanuise, J. P. Villian, R. G. Greenwald, P. T. Newell, and F. J. Rich, Correlated observations of the boundary between polar cap and nightside auroral zone by HF radars and the DMSP satellite, *Geophys. Res. Lett.*, 21, 221, 1994.
56. Takahashi, K., B. J. Anderson, P. T. Newell, T. Yamamoto, N. Sato, Propagation of Pc 3 pulsations from space to the ground: A case study using multipoint measurements, submitted to *AGU Monograph on Solar Wind Sources of Magnetospheric ULF Waves*, 1993.
57. Velosky, I., P. T. Newell, and A. T. Y. Lui, Pervasive small-scale enhancements in mantle and polar rain precipitation, *Geophys. Res. Lett.*, 22, 3263-3266, 1995.
58. Watanabe, M., T. Iijima, M. Nakagawa, T. A. Potemra, S. Ohtani, and P. T. Newell, Dayside field-aligned current system during vanishingly small IMF condition, submitted to *J. Geophys. Res.*, 1995.
59. Watermann, J., O. de la Beaujardiere, D. Lummerzheim, P. T. Newell, and F. J. Rich, The ionospheric footprint of magnetosheath-like particle precipitation observed by an incoherent scatter radar, submitted to *JGR*, 1993.

60. Watermann, J., O. de la Beaujardiere, and P. T. Newell, Incoherent scatter observations of ionospheric signatures of cusp-like electrons, *J. Geomag. Geoelectr.*, 44, 1195, 1992.
61. Wing, S., P. T. Newell, D. G. Sibeck, and K. B. Baker, A large statistical study of the entry of interplanetary magnetic field Y-component into the magnetosphere, *Geophys. Res. Lett.*, 22, 2083-2086, 1995.
62. Wing, S., P. T. Newell, and T. G. Onsager, Modeling the entry of magnetosheath electrons into the dayside ionosphere, submitted to *J. Geophys. Res.*, 1995.
63. Xu, D., M. G. Kivelson, R. J. Walker, P. T. Newell, and C.-I. Meng, Interplanetary magnetic field control of mantle precipitation and associated field-aligned currents, *J. Geophys. Res.*, 100, 1837-1846, 1995.
64. Yamamota, T., K. Makita, and C.-I. Meng, A particle simulation of the westward traveling surge, *J. Geophys. Res.*, 98, 13653, 1993.
65. Yamamota, T. K. Makita, and C.-I. Meng, A particle simulation of 'Giant' undulations on the evening diffuse auroral boundary, *J. Geophys. Res.*, 98, 5785-5800, 1993.